Bioscience, Biotechnology, and Biochemistry, 2025, **89**, 805–810
https://doi.org/10.1093/bbb/zbaf030
Advance access publication date: 8 March 2025
Regular Paper

Six-step synthesis and epithelial-mesenchymal transition–inhibitory activity of a tetralone-based vitetrifolin analog

Yusuke Hanaki*, Yasunori Sugiyama, and Ryo C. Yanagita

Department of Applied Biological Science, Faculty of Agriculture, Kagawa University, Kagawa, Japan
*Correspondence: Yusuke Hanaki, hanaki.yusuke@kagawa-u.ac.jp

Abstract

We synthesized a vitetrifolin analog in which the A-ring was replaced with a benzene ring, in 6 steps from commercially available 2-methyl-1-tetralone. Similarly to vitetrifolin D, this analog suppressed the phorbol ester–induced epithelial-mesenchymal transition. This tetralone-based structural simplification strategy is expected to be applicable to studies on not only vitetrifolins but also other halimane-type diterpenoids.

Keywords: vitetrifolin, simplified analog, epithelial-mesenchymal transition

Graphical abstract

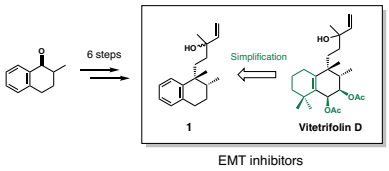

A tetralone-based vitetrifolin analog (**1**) was synthesized in 6 steps. It inhibited phorbol ester–induced EMT similarly to vitetrifolin D.

Plants in the genus *Vitex*, such as *V. rotundifolia* (beach vitex), *V. agnus-castus* (chastetree), and *V. trifolia* (simple-leaf chastetree), have traditionally been used as herbal medicines to relieve pain and inflammation (Das *et al.* 2022). In particular, the fruit of *V. agnus-castus* has been used to treat gynecological issues such as menstrual pain, dysmenorrhea, and endometriosis (Mayo 1998; Farzaei, Niroumand and Heydarpour 2018). The vitetrifolins (Figure 1) isolated from these plants are halimane-type diterpenoids with unique biological activities (Ono, Ito and Nohara 2001; Wu *et al.* 2009). For example, vitetrifolin D has been found to suppress lipopolysaccharide-induced nitric oxide production (Lee *et al.* 2013) and the hedgehog signaling pathway (Arai *et al.* 2013), whereas vitetrifolin F has been found to inhibit α-glucosidase activity (Djimabi *et al.* 2022). We recently found that vitetrifolin D can inhibit the phorbol ester–induced decrease in E-cadherin levels in HHUA endometrial cells (Hanaki *et al.* 2023). The loss of E-cadherin triggers the epithelial-mesenchymal transition (EMT), resulting in cell invasion and metastasis in cancer and endometriosis (Yang and Yang 2017). Thus, vitetrifolin D is thought to contribute to the medicinal efficacy of *Vitex* plants. The mode of action and the *in vivo* efficacy of vitetrifolin D should be investigated, but the limited availability of this compound in plants has hampered such studies. Moreover, neither the total synthesis nor the semisynthesis of vitetrifolins has been achieved. One reason for this lack is the difficulty of stereoselective construction of the 8-*epi*-halim-5(10)-ene skeleton of vitetrifolins (Roncero *et al.* 2018; Quilez Del Moral *et al.* 2019). The semisyntheses of some *ent*-halimane-type diterpenoids from *ent*-halimic acid, which is abundant in *Halimium viscosum*, have been reported (Roncero *et al.* 2018). However, the isolation of diterpenoids from plants still requires time and effort, and 8-*epi*-halim-5(10)-ene derivatives have not been isolated in a sufficient quantity for use as a starting material.

To address this supply problems, we attempted to develop a simplified vitetrifolin analog that retained EMT-inhibitory activity. Because the chain structure between positions 11 and 15, including a terminal alkene and tertiary alcohol groups, is characteristic of vitetrifolins, we predicted that this structure is essential for their biological activities. In contrast, the A-ring structure is common among many other diterpenes that lack biological activity, suggesting that the A-ring may not be necessary for the biological activity of vitetrifolins. The acyl groups at positions 6 and 7 differ among vitetrifolins, but they are thought to be immediately hydrolyzed by esterases in cells (Lavis 2008). Because the two hydroxy groups resulting from hydrolysis can form a hydrogen bond with each other, they might not be involved in the interaction with intracellular target proteins. We speculated that the acetyl groups contributed to increasing in molecular hydrophobicity and cell

Received: 30 January 2025; **Accepted:** 5 March 2025

permeability, resulting that only vitetrifolin D was identified as an EMT inhibitor among vitetrifolins (Hanaki *et al.* 2023). To test these hypotheses, we synthesized and evaluated the EMT-inhibitory activity of a simplified analog **1**, in which the acetoxy groups were removed and the A-ring was replaced with a benzene ring to increase the synthetic accessibility. Because the lipophilicity of **1** estimated via molinspiration cheminformatics software (Molinspiration Cheminformatics, 2025) was similar to that of vitetrifolin D (miLogP of **1**, 4.78; and of vitetrifolin D, 5.10), we estimated that this structural simplification would not drastically affect the cell permeability nor number of nonspecific interactions with intracellular substances.

Results and discussion

Synthesis of a tetralone-based vitetrifolin analog (1)

Compound **1** was synthesized as racemates from commercially available 2-methyl-1-tetralone (Scheme 1). First, 2-methyl-1-tetralone was converted to racemic **3** according to a previously reported protocol (Kong *et al.* 2024). The reaction of this ketone with CH_2I_2 and MeLi generated an epoxide, and subsequent Meinwald-type 1,2-H migration afforded aldehyde **2** (Li *et al.* 2019). The quaternary carbon center of **3** was formed by α-methylation with iodomethane in the presence of potassium *tert*-butoxide. Nuclear magnetic resonace (NMR) spectra of **3** were in good agreement with the literature data (Kong *et al.* 2024). However, the Horner-Wadsworth-Emmons reaction of **3** with dimethyl (2-oxopropyl) phosphonate did not proceed, likely because of steric hindrance. Fortunately, the aldol reaction with acetone in the presence of sodium methoxide (Maugel *et al.* 2010) afforded α,β-unsaturated ketone **4**, albeit in low yield. Although the yield could be increased by using other bases (Buter *et al.* 2016), we proceeded with the next step because a sufficient amount of **4** was obtained. Palladium-catalyzed hydrogenation of **4** successfully afforded **5**. Finally, the addition of a vinyl group to the ketone via the Grignard reaction afforded **1** as a 1:1 mixture of diastereomers at position 13, but they could not be separated by column chromatography. Previously, total synthesis of nakamurol A and 3β-hydroxymanool, labdane-type diterpenoids that have the same chain structure with vitetrifolins, has been reported (Bonjoch *et al.* 2000; Díaz *et al.* 2003; Justica *et al.* 2004). They were also synthesized as a mixture of diastereomers at position 13. The diastereomers of nakamurol A could not be separated (Bonjoch *et al.* 2000; Díaz *et al.* 2003), while those of 3β-hydroxymanool were easily separated by flash chromatography (Justica *et al.* 2004). Thus, the separability of these diastereomers might depend on their overall structure, and some derivatizations might be necessary to separate the diastereomers of **1**. Moreover, the stereochemistry at position 13 of vitetrifolin D has not been determined (Ono, Ito and Nohara 2001). Therefore, we in this study subjected **1** to the following biological assays without separation of the diastereomers to immediately evaluate its biological activities.

Cytotoxicity of 1

First, the cytotoxicity of **1** against HHUA endometrial cells was evaluated by means of a WST-based colorimetric assay (Figure 2), and the IC_{50} value was found to be 6.3 μM. Cytotoxicity of **1** could not be simultaneously compared to that of vitetrifolin D because we have isolated only an extremely small amount of vitetrifolin D (Hanaki *et al.* 2023). However, **1** was estimated to be several times more cytotoxic than vitetrifolin D, as the viability of HHUA cells at the presence of 9 μM of vitetrifolin D was 58% in an assay under the same condition (Hanaki *et al.* 2023).

EMT-inhibitory activity of 1

We next evaluated the EMT-inhibitory activity of **1** in HHUA cells. Our previous study revealed that 12-*O*-tetradecanoylphorbol 13-acetate (TPA), a protein kinase C activator, induced the EMT in HHUA cells (Hanaki *et al.* 2022). Specifically, TPA decreased the content of E-cadherin, a major component of the epithelial adherens junction, and increased the content of vimentin, an intermediate filament of mesenchymal cells. At concentrations of 3-9 μM, vitetrifolin D suppressed the TPA-induced decrease in E-cadherin content and consequently decreased the vimentin/E-cadherin ratio (Hanaki *et al.* 2023). Thus, we evaluated whether **1** inhibited the TPA-induced change in the levels of these EMT marker proteins. Since cell viability was markedly decreased at the presence of 10-30 μM of **1** (Figure 2), it was difficult to collect enough amount of proteins from cells treated with these concentrations of **1**. Adjustment of protein concentration of individual collected samples was also difficult, because HHUA cells were cultured on collagen gels and they were collectively lysed and subjected to sodium dodecyl sulfate-polyacrylamide gel electrophoresis (SDS-PAGE) (Hanaki *et al.* 2022). Thus, we tested the EMT-inhibitory activity of **1** at 1-3 μM. As shown in Figure 3, the vimentin/E-cadherin ratio tended to decrease dose-dependently in the presence of **1**. Although **1** exhibited weak cytotoxicity at 3 μM (Figure 2), we concluded that the observed effect could not be attributed merely to cytotoxicity but also resulted from EMT suppression, as another diterpenoids decreased cell viability without any effect on the levels of EMT marker proteins (Hanaki *et al.* 2024). To summarize the above results, **1** exhibited EMT-inhibitory activity comparable to or greater than that of vitetrifolin D.

Conclusions

In this study, we synthesized a simplified vitetrifolin analog (**1**) that inhibited the TPA-induced EMT. Because **1** was prepared as a racemic mixture of diastereomers at position 13, the biological activities of each isomer remained uncertain. In addition, the aldol reaction of **3** with acetone was not optimized. However, despite these limitations, **1** was synthesized in only 6 steps with a yield of at least several tens of milligrams. The synthetic accessibility of this compound is expected to be advantageous for future biological studies on vitetrifolins. Future studies will focus on the EMT-inhibitory mechanism and other potential vitetrifolin-like biological activities, such as anti-inflammatory and hedgehog signaling pathway–inhibitory activities (Arai *et al.* 2013; Lee *et al.* 2013) of **1**. We will also try to synthesize **1** enantio- and diastereo-selectively and identify a stereoisomer with superior EMT-inhibitory activity. Asymmetric protonation of the enolate can afford both enantiomers of 2-methyl-1-tetralone (Oudeyer, Brière and Levacher 2014). In addition, the tertiary alcohol group at position 13 could be stereo-selectively constructed by using asymmetric epoxidation as a key step (Díaz *et al.* 2003). Therefore, all enantiomers and diastereomers of **1** would be individually prepared in the future.

Notably, the prepared tetralone-based analog, whose A-ring was replaced with a benzene ring, retained an EMT-inhibitory activity comparable to that of vitetrifolin D. Since the functional groups on the B-ring of halimane-type diterpenoids are more varied than those on the A-ring, the unique biological properties of

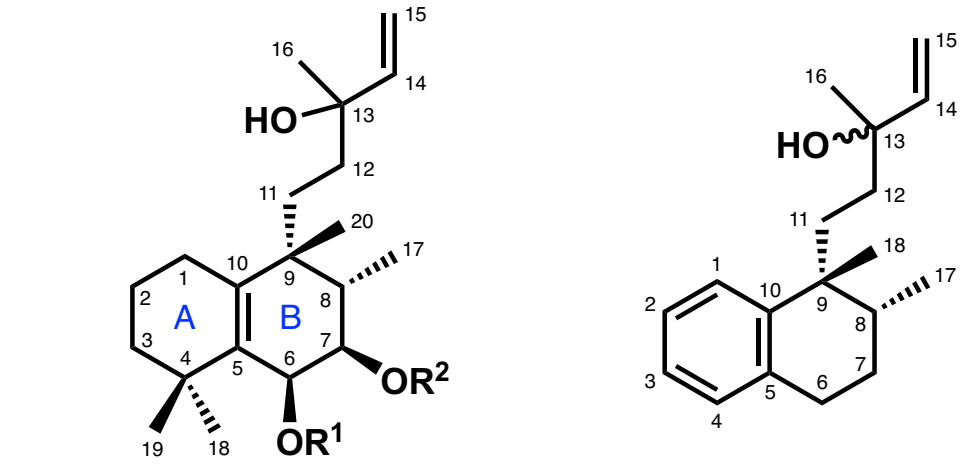

Figure 1. Structure of vitetrifolins and **1**.

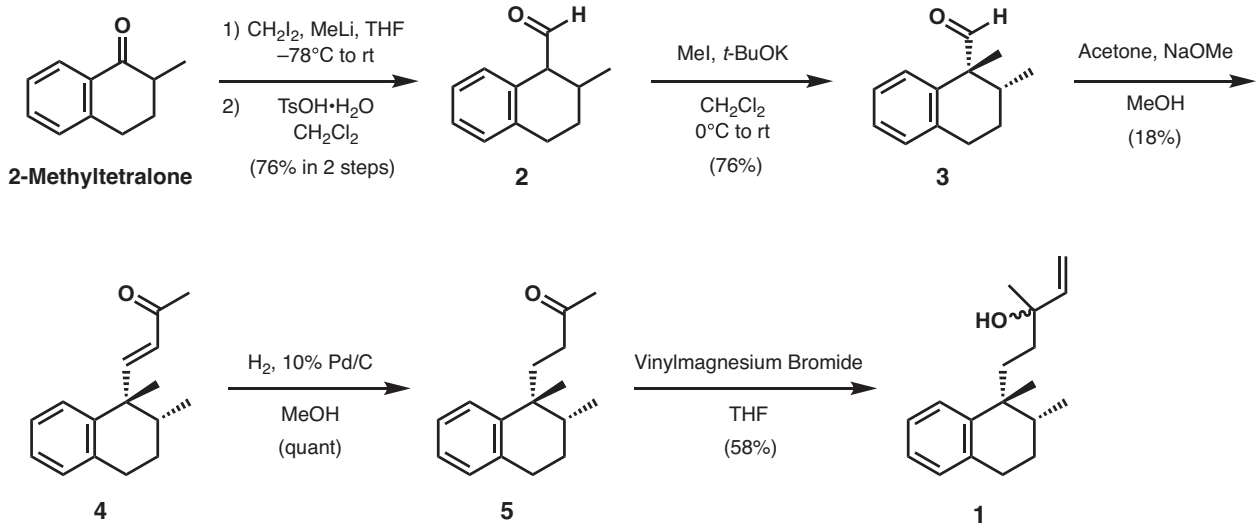

Scheme 1. Synthesis of **1**.

each derivative can be attributed to the partial structure excluding the A-ring. We have recently started to synthesize tetralone-based analogs of other halimane-type diterpenoids. Because the benzene rings in these compounds can easily be functionalized, it is likely that a molecular probe based on these analogs could be readily developed. Therefore, our new analogs are expected to facilitate future research on the mode of action and *in vivo* efficacy of halimane-type diterpenoids.

Experimental

General remark

NMR spectra were recorded on JNM-ECZ500 (JEOL, Tokyo, Japan), and chemical shifts are reported in ppm relative to the residual solvent (^{1}H NMR: $CDCl_3$ as $\delta = 7.26$ ppm and acetonitrile-d3 as $\delta = 1.93$ ppm, ^{13}C NMR: $CDCl_3$ as $\delta = 77.0$ ppm and acetonitrile-d3 as $\delta = 1.30$ ppm). High-resolution electrospray ionization mass spectra (HR-ESI-qTOF-MS) were recorded on a micrOTOF II (Brucker Daltonics, Billerica, MA, USA). Wakogel C-300 (FUJIFILM Wako Pure Chemical Corporation, Osaka, Japan) was used for column chromatography. All other reagents were purchased from chemical companies and used without further purification.

Synthesis of 3

Compound **3** was synthesized as reported previously (Kong *et al.* 2024).

^{1}H NMR (500 MHz, acetonitrile-d3) δ 1.05 (3H, d, $J = 6.9$ Hz), 1.40 (3H, s), 1.85-1.95 (3H, m), 2.86-2.90 (2H, m), 7.02 (1H, m), 7.14-7.19 (3H, m), 9.66 (1H, s).

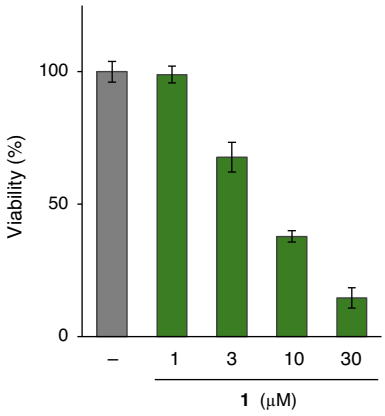

Figure 2. Cytotoxicity of **1** against HHUA endometrial cells. HHUA cells were treated with the indicated concentrations of **1** for 24 h. Thereafter, the cell viability was determined via the WST assay. The cell viability was expressed as a percentage relative to that of the vehicle group. The error bars represent the SE ($n = 4$).

^{13}C NMR (125 MHz, acetonitrile-d3) δ 16.8, 22.5, 28.8, 29.7, 38.8, 53.8, 127.3, 127.8, 129.7, 130.6, 137.3, 139.1, 204.1.

Synthesis of 4

To a solution of **3** (144 mg, 0.766 mmol) in acetone (0.89 mL) was added 5 M NaOMe in MeOH (0.77 mL, 3.85 mmol, 5 equiv) at room temperature. After stirring for 24 h at room temperature, the reaction was quenched with H_2O (2 mL) and saturated aq NH_4Cl (5 mL). The mixture was extracted with EtOAc (10 mL × 3). The combined organic layer was washed with brine, dried over Na_2SO_4, filtered, and concentrated *in vacuo*. The residue was purified by column chromatography (silica gel, 1% → 3% EtOAc/hexane) to afford **4** (30.7 mg, 0.135 mmol, 18%) as a yellow oil.

^{1}H NMR (500 MHz, $CDCl_3$) δ 1.00 (3H, d, $J = 6.9$ Hz), 1.50 (3H, s), 1.62 (1H, m), 1.76 (1H, m), 1.84 (1H, m), 2.22 (3H, s), 2.83-2.87 (2H, m), 5.88 (1H, d, $J = 16.6$ Hz), 6.93 (1H, d, $J = 16.6$ Hz), 7.08-7.14 (4H, m).

^{13}C NMR (125 MHz, $CDCl_3$) δ 17.2, 25.8, 27.1, 27.5, 29.5, 40.0, 44.2, 126.1, 126.2, 128.7, 129.3, 129.7, 136.5, 140.9, 153.9, 198.9.

HR-ESI-MS (ESI, positive): $C_{16}H_{20}NaO$ (M + Na) 251.1406; found 251.1406.

Synthesis of 5

To a solution of **4** (26.5 mg, 0.116 mmol) in MeOH (3 mL) was added 10% Pd/C (15.0 mg) at room temperature. The mixture was vigorously stirred under an H_2 atmosphere at room temperature for 3 h. The mixture was filtered, and the filtrate was concentrated *in vacuo* to afford **5** (27.0 mg, 0.116 mmol, quant) as a colorless oil.

^{1}H NMR (500 MHz, $CDCl_3$) δ 1.02 (3H, d, $J = 6.9$ Hz), 1.28 (3H, s), 1.62-1.84 (4H, m), 1.91 (1H, ddd, $J = 14.0$, 11.5, 5.5 Hz), 2.06 (3H, s), 2.26-2.39 (2H, m), 2.78-2.85 (2H, m), 7.06-7.15 (3H, m), 7.30 (1H, d, $J = 8.1$ Hz).

^{13}C NMR (125 MHz, $CDCl_3$) δ 16.2, 27.1, 28.0, 28.4, 30.0, 31.0, 38.2, 38.9, 39.9, 125.5, 125.5, 126.8, 129.2, 136.4, 143.5, 209.3.

HR-ESI-MS (ESI, positive): $C_{16}H_{22}NaO$ (M + Na) 253.1563; found 253.1566.

Synthesis of 1

To a solution of **5** (23.8 mg, 0.103 mmol) in tetrahydrofuran (THF) (0.50 mL) was added 1 M vinyl magnesium bromide in THF (0.16 mL, 0.160 mmol, 1.6 equiv) at 0 °C. The mixture was stirred at 0 °C for 30 min and at room temperature for 30 min. The reaction was quenched with saturated aq NH_4Cl (2 mL). The mixture was extracted with EtOAc (2 mL × 4). The combined organic layer was washed with brine, dried over Na_2SO_4, filtered, and concentrated *in vacuo*. The residue was purified by column chromatography (silica gel, 2.5% EtOAc/hexane) to afford **1** (15.3 mg, 59.3 μmol, 58%, 1:1 diastereomixture at C13) as a colorless oil.

^{1}H NMR (500 MHz, $CDCl_3$) δ 0.99 (0.5 × 3H, d, $J = 6.9$ Hz, H_3-17), 1.01 (0.5 × 3H, d, $J = 6.9$ Hz, H_3-17), 1.22 (0.5 × 3H, s, H_3-16), 1.23 (0.5 × 3H, s, H_3-16), 1.26 (3H, s, H_3-18), 1.31-1.58 (3H, m, H-11a, H-12a, H-12b), 1.63-1.85 (4H, m, H-7a, H-7b, H-8, H-11b), 2.73-2.88 (2H, m, H-6a, H-6b), 5.03 (1H, d, $J = 10.8$ Hz, H-15a), 5.16 (1H, d, $J = 17.8$ Hz), 5.81 (0.5 × 1H, dd, $J = 17.8$, 10.3 Hz, H-14), 5.82 (0.5 × 1H, dd, $J = 17.2$, 10.9 Hz, H-14), 7.03-7.10 (2H, m, H-3, H-4), 7.13 (1H, m, H-2), 7.30 (1H, m, H-1).

^{13}C NMR (125 MHz, $CDCl_3$) δ 16.1 (0.5 × 1C, C-17), 16.1 (0.5 × 1C, C-17), 27.1 (0.5 × 1C, C-7), 27.2 (0.5 × 1C, C-7), 27.6 (0.5 × 1C, C-16), 27.8 (0.5 × 1C, C-16), 28.2 (0.5 × 1C, C-6), 28.3 (0.5 × 1C, C-6), 28.9 (0.5 × 1C, C-18), 29.1 (0.5 × 1C, C-18), 31.8 (0.5 × 1C, C-11), 31.9 (0.5 × 1C, C-11), 37.3 (0.5 × 1C, C-12), 37.4 (0.5 × 1C, C-12), 37.8 (0.5 × 1C, C-8), 37.8 (0.5 × 1C, C-8), 39.0 (0.5 × 1C, C-9), 39.1 (0.5 × 1C, C-9), 73.4 (0.5 × 1C, C-13), 73.5 (0.5 × 1C, C-13), 111.8 (1C, C-15), 125.2 (1C, C-3), 125.5 (1C, C-2), 126.7 (0.5 × 1C, C-1), 126.7 (0.5 × 1C, C-1), 129.1 (1C, C-4), 136.3 (0.5 × 1C, C-5), 136.4 (0.5 × 1C, C-5), 144.4 (0.5 × 1C, C-10), 144.4 (0.5 × 1C, C-10), 144.9 (0.5 × 1C, C-14), 145.0 (0.5 × 1C, C-14).

HR-ESI-MS (ESI, positive): $C_{18}H_{26}NaO$ (M + Na) 281.1876; found 281.1878.

Cell culture

HHUA (RCB0658) human endometrial cancer cell line was provided by RIKEN BRC through National Bio-Resource Project of the NEXT/AMED (Tsukuba, Japan). HHUA cells were cultured in Ham's F-12 medium with 10% heat-inactivated fetal bovine serum (FBS), 1 mM L-glutamine, 100 U/mL penicillin, and 100 μg/mL streptomycin. They were maintained at 37 °C in a humidified atmosphere containing 5% CO_2.

Cytotoxicity assay

HHUA cells (1×10^4 cells/200 μL·well) were seeded in a 96-well plate and allowed to attach overnight. Thereafter, solution of **1** in dimethyl sulfoxide (DMSO) or DMSO alone was added. After incubation for 24 h, 20 μL of Cell Counting Kit-8 (FUJIFILM Wako Pure Chemical Corporation, Osaka, Japan) was added to each well, and the plate was incubated at 37 °C for an additional 4 h. The absorbance at 450 nm was measured for the control (*C*) well and the test well (*T*) using a microplate reader (Multiskan FC; Thermo Fisher Scientific, Walthman, MA, USA). Cell viability in the presence of each concentration (1, 3, 10, and 30 μM) of **1** was calculated as 100 × (*T*/*C*) using average of quadruplicate points. IC_{50} value, defined as 100 × (*T*/*C*) = 50, was determined by processing these values.

Western blotting

To each well of a 48-well plate, 0.25% of atelocollagen solution (KOKEN Co., Ltd, Tokyo, Japan) was added (150 μL/well) and incubated at 37 °C for 3 h to allow gelation. HHUA cells (7.5×10^4 cells/450 μL·well) were seeded in a collagen gel-coated 48-well plate and allowed to attach overnight, and then solution of **1** in DMSO or DMSO alone was added. After incubation for 30 min, TPA solution in DMSO or DMSO alone was added and incubated for 16 h. Cells and collagen gels were washed with PBS, lysed by

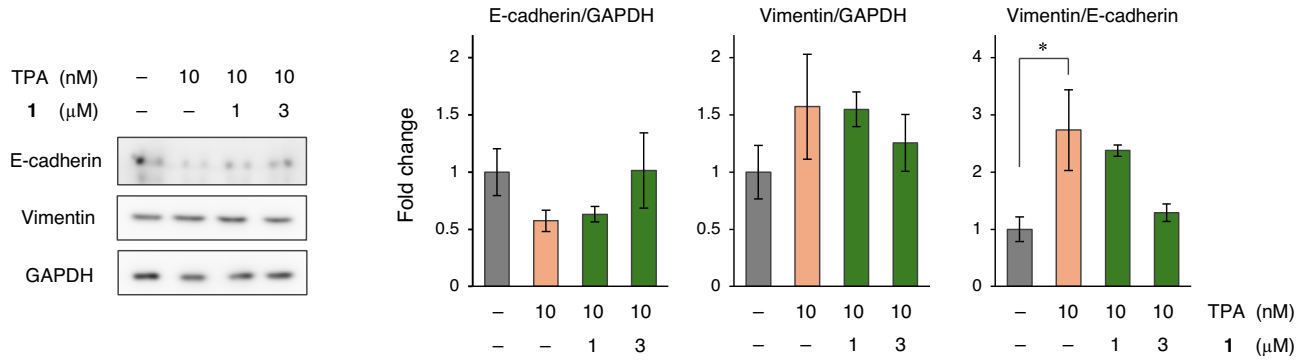

Figure 3. EMT-inhibitory activity of **1**. HHUA cells cultured on collagen type I gels were first treated with the indicated concentrations of **1** and then treated with TPA for 16 h. Thereafter, the cells were lysed, an equal amount of each lysate was separated by SDS-PAGE, and the EMT marker proteins were analyzed by western blotting. A representative result of western blotting and quantification of the band intensities from triplicate samples are shown. The error bars represent the SE ($n = 3$). *$P < .05$ (Tukey's test).

adding 100 μL of 2X SDS sample buffer, and boiled for 10 min. Equal amounts of sample were subjected to SDS-PAGE using slab gels consisting of a 10% acrylamide separation gel and a 3% stacking gel, and transferred to a nitrocellulose membrane. After blocking with PBS-T containing 0.5% skimmed milk for 1 h at room temperature, the blots were incubated for 2 h at room temperature with primary antibodies. After washing with PBS-T, the blots were incubated for 1 h at room temperature with secondary antibodies. After washing, the chemiluminescence signal of each band was quantified using Amersham Imager 680 analysis software (GE healthcare, Chicago, IL, USA). Anti-E-cadherin (24E10), anti-vimentin (D21H3), anti-GAPDH (D16H11), and HRP-conjugated anti-rabbit IgG antibodies were obtained from Cell Signaling Technology (Danvers, MA, USA). These antibodies were diluted 1:1000 and used for the detection of immunoreactive bands.

Supplementary material

Supplementary material is available at *Bioscience, Biotechnology, and Biochemistry* online.

Data availability

The data underlying this study are available in the published article and its online supplementary material.

Author contribution

Y.H.: conceptualization, writing original draft, methodology, investigation, and analysis. Y.S.: editing, investigation, and analysis. R.C.Y.: editing, methodology, and analysis.

Funding

This work was supported by the Japan Society for the Promotion of Science (JSPS) KAKENHI (grant number 24K17837 to Y.H.).

Disclosure statement

No potential conflict of interest was reported by the authors.

Acknowledgments

The authors thank Ms Tsugumi Shiokawa and Dr Hiroko Tada (Okayama University) for MS measurement.

References

Arai MA, Fujimatsu T, Uchida K *et al.* Hh signaling inhibitors from Vitex negundo; naturally occurring inhibitors of the GLI1-DNA complex. *Mol BioSyst* 2013;**9**:1012-8. https://doi.org/10.1039/c3mb25567k

Bonjoch J, Cuesta J, Dı´az S *et al.* Total synthesis of (±)-nakamurol-A and its 13-epimer: tentative assignment of the C-13 relative configuration. *Tetrahedron Lett* 2000;**41**:5669-72. https://doi.org/10.1016/S0040-4039(00)00885-6

Buter J, Heijnen D, Wan IC *et al.* Stereoselective synthesis of 1-tuberculosinyl adenosine: a virulence factor of *Mycobacterium tuberculosis*. *J Org Chem* 2016;**81**:6686-96. https://doi.org/10.1021/acs.joc.6b01332

Das N, Salgueiro ACF, Choudhury DR *et al.* Traditional uses, phytochemistry, and pharmacology of genus *Vitex* (Lamiaceae). *Phytother Res* 2022;**36**:571-671. https://doi.org/10.1002/ptr.7330

Díaz S, Cuesta J, González A *et al.* Synthesis of (-)-nakamurol A and assignment of absolute configuration of diterpenoid (+)-nakamurol A. *J Org Chem* 2003;**68**:7400-6. https://doi.org/10.1021/jo034838r

Djimabi K, Wang R-Y, Li B *et al.* Diterpenoids with α-glucosidase inhibitory activities from the fruits of *Vitex trifolia*. *Fitoterapia* 2022;**161**:105248. https://doi.org/10.1016/j.fitote.2022.105248

Farzaei M, Niroumand M, Heydarpour F. Pharmacological and therapeutic effects of *Vitex agnus-castus L.*: a review. *Pharmacogn Rev* 2018;**12**:103. https://doi.org/10.4103/phrev.phrev_22_17

Hanaki Y, Abe R, Sugiyama Y *et al.* A new labdane-type diterpenoid from leaves of *Vitex rotundifolia*. *Results Chem* 2024;**7**:101512. https://doi.org/10.1016/j.rechem.2024.101512

Hanaki Y, Iwase N, Sugiyama Y *et al.* Cell morphology-based screening identified vitetrifolin D from *Vitex rotundifolia* as an inhibitor of phorbol ester-induced downregulation of E-cadherin in HHUA endometrial cells. *BPB Reports* 2023;**6**:103-7. https://doi.org/10.1248/bpbreports.6.3_103

Hanaki Y, Miyoshi S, Sugiyama Y *et al.* 12-O-tetradecanoylphorbol 13-acetate promotes proliferation and epithelial-mesenchymal transition in HHUA cells cultured on collagen type I gel: a feasible model to find new therapies for endometrial diseases. *Biosci Biotechnol Biochem* 2022;**86**:1417-22. https://doi.org/10.1093/bbb/zbac136

Justicia J, Rosales A, Buñuel E *et al.* Titanocene-catalyzed cascade cyclization of epoxypolyprenes: straightforward synthesis of terpenoids by free-radical chemistry. *Chem Eur J* 2004;**10**:1778-88. https://doi.org/10.1002/chem.200305647

Kong L, Gan X-C, van der Puyl Lovett VA *et al.* Alkene hydrobenzylation by a single catalyst that mediates iterative outer-sphere steps. *J Am Chem Soc* 2024;**146**:2351-7. https://doi.org/10.1021/jacs.3c13398

Lavis LD. Ester bonds in prodrugs. *ACS Chem Biol* 2008;**3**:203-6. https://doi.org/10.1021/cb800065s

Lee C, Lee JW, Jin Q *et al.* Anti-inflammatory constituents from the fruits of *Vitex rotundifolia*. *Bioorg Med Chem Lett* 2013;**23**:6010-4. https://doi.org/10.1016/j.bmcl.2013.08.004

Li Y, Han J, Luo H *et al.* Access to benzylic quaternary carbons from aromatic ketones. *Org Lett* 2019;**21**:6050-3. https://doi.org/10.1021/acs.orglett.9b02204

Maugel N, Mann FM, Hillwig ML *et al.* Synthesis of (±)-nosyberkol (isotuberculosinol, revised structure of edaxadiene) and (±)-tuberculosinol. *Org Lett* 2010;**12**:2626-9. https://doi.org/10.1021/ol100832h

Mayo JL. Black cohosh and chasteberry: herbs valued by women for centuries. *Clin Nutr Insight* 1998;**6**:1-4.

Molinspiration Cheminformatics. 2025. https://www.molinspiration.com/ (3 January 2025, date last accessed).

Ono M, Ito Y, Nohara T. Four new halimane-type diterpenes, vitetrifolins D-G, from the fruit of Vitex trifolia. *Chem Pharm Bull* 2001;**49**:1220-2. https://doi.org/10.1248/cpb.49.1220

Oudeyer S, Brière J-F, Levacher V. Progress in catalytic asymmetric protonation. *Eur J Org Chem* 2014;**2014**:6103-19. https://doi.org/10.1002/ejoc.201402213

Quilez Del Moral JF, Domingo V, P Á *et al.* Mimicking halimane synthases: monitoring a cascade of cyclizations and rearrangements from epoxypolyprenes. *J Org Chem* 2019;**84**:13764-79. https://doi.org/10.1021/acs.joc.9b01996

Roncero AM, Tobal IE, Moro RF *et al.* Halimane diterpenoids: sources, structures, nomenclature and biological activities. *Nat Prod Rep* 2018;**35**:955-91. https://doi.org/10.1039/C8NP00016F

Wu J, Zhou T, Zhang S-W *et al.* Cytotoxic terpenoids from the fruits of *Vitex trifolia* L. *Planta Med* 2009;**75**:367-70. https://doi.org/10.1055/s-0028-1112211

Yang Y-M, Yang W-X. Epithelial-to-mesenchymal transition in the development of endometriosis. *Oncotarget* 2017;**8**:41679-89. https://doi.org/10.18632/oncotarget.16472

Received: 30 January 2025. **Accepted:** 5 March 2025